Nigerian Research Journal of Chemical Sciences (ISSN: 2682-6054)
Volume 13, Issue 2, 2025

Properties of Plaster of Paris, Waste Polyethylene Terephthalate and Glass Fiber Composite

[*]Kaloma A. Musa, and Musa Esther Turu

Department of Chemical Sciences, Federal University, Kashere, Gombe State, Nigeria.

*Corresponding Author: musakalomaadamu@gmail.com

Accepted: *August 23, 2025.* **Published Online***: December 8, 2025*

ABSTRACT

This study investigates the morphological properties of Plaster of Paris (POP) composites reinforced with waste polyethylene terephthalate (PET) and glass fibers as a sustainable approach to improving mechanical performance while addressing solid waste challenges. Raw gypsum was processed to obtain POP and subsequently blended with varying proportions of PET and glass fibers. The composites were characterized using Scanning Electron Microscopy (SEM) and Fourier Transform Infrared (FTIR) spectroscopy to evaluate microstructural behavior, interfacial interactions, and functional group modifications. SEM analysis revealed that low fiber loadings promoted uniform dispersion of PET and glass within the gypsum matrix, enhancing stress transfer, reducing porosity, and improving tensile and flexural strength. However, higher fiber concentrations led to agglomeration, void formation, and heterogeneous structures, which introduced stress concentration sites and reduced mechanical performance. FTIR spectra confirmed the coexistence of gypsum, PET, and glass phases, with overlapping sulfate and silicate bands indicating partial interfacial interactions rather than strong chemical bonding. Overall, the incorporation of PET and glass fibers reduced brittleness, improved toughness, and decreased porosity, demonstrating the potential of hybrid POP-based composites for construction and decorative applications. The findings highlight the dual environmental benefit of recycling plastic and glass waste while enhancing the functional properties of POP materials.

Keywords: Composite materials, glass fiber, morphology, plaster of paris, polyethylene terephthalate, solid waste recycling.

INTRODUCTION

Plaster of Paris (POP, $CaSO_4.1/2H_2O$), also known as calcined gypsum, is a form of plaster derived from gypsum ($CaSO_4 \cdot 2H_2O$), a mineral commonly found in sedimentary rocks [1] use

number for references in the text The name originates from the large gypsum deposit s near Paris, heavily mined in the 18th century. Historically, gypsum has been widely used as a construction material, surgical plaster, and for making ceramic molds, with evidence of its application dating back to ancient Egypt, where it was employed in pyramid construction. POP is produced by heating gypsum to about 120–180 °C [1, 2]. POP is valued for its rapid setting, smooth finish, non-toxicity, low thermal conductivity, and fire-retardant properties, making it ideal for decorative works, moldings, and architectural designs [3].

Composites are materials formed by combining two or more distinct substances to achieve enhanced properties [4]. Among them, fiber-reinforced composites are widely used, in which fibers such as carbon or glass strengthen a polymer or metal matrix by providing stiffness, while the matrix binds and transfers loads. Composites are increasingly favored because they are lighter, stronger, more durable, and often cheaper compared to conventional materials [5]

Polyethylene terephthalate is one of the most widely produced thermoplastic polymers [6]. In the United States, PET is the most recycled plastic, yet only about 20% of it undergoes effective recycling. Commonly used in bottles and containers, PET can be reprocessed into fibers for carpets or fiberfill, or chemically broken down and re-synthesized into new PET. Since the 1970s, advancements in stretch-molding enabled PET to be made into strong, clear beverage bottles, which became its second-largest application after fibers [7] Due to its favorable physicochemical, thermal, and mechanical properties, PET has been investigated for improving POP composites. Its ability to form emulsions, disperse as solid particles, and develop gels or micelles makes it a suitable additive for enhancing the strength and performance of plaster [8].

Glass is primarily composed of silica, soda, and lime, with silica commonly sourced from quartz sand, while soda ash (Na_2CO_3) and limestone ($CaCO_3$) supply Na_2O and CaO. Additional materials may be introduced to modify color or impart special properties. Based on chemical composition, glasses are classified into types such as vitreous silica, alkali silicates, soda-lime, borosilicate, lead, barium, and aluminosilicate glasses. Soda-lime glass, which contains about 73% SiO_2, 13% Na_2O, and 10% CaO, is the most widely used, particularly in containers, sheet glass, and float glass, and also exhibits pozzolanic-cementitious characteristics. Lead glass represents another major category, commonly applied in electronics, neon tubing, and television screens [9] Waste glass consists predominantly of soda-lime glass, with about 63% being clear,

25% amber, 10% green, and 2% other colors. Naturally, glass forms when silicate-rich rocks melt at high temperatures and cool rapidly before crystallization occurs [9]

Globally, waste glass generation is rising with industrialization and urbanization. In the United States, 11,530 kilotons were produced in 2010, but only 27.1% was recycled, primarily for containers and packaging [10]. Similarly, in 2005, 12.8 million tons of waste glass were generated, while only 2.75 million tons were recycled. In Malaysia, three manufacturers produce 600 tons of glass bottles daily, yet only 10% is reused. In Poland, about 900,000 tons of glass waste were produced in 2004, with 300,000 tons recycled [10] Major sources of glass waste include bottles, windowpanes, screens, bulbs, electronic parts, and medical containers [9] Due to high cleaning and sorting costs, only a small fraction is recycled, resulting in lower recycling rates compared to other solid wastes.

Solid waste in general remains a pressing global issue, with projections indicating municipal solid waste will rise by 70% by 2050, reaching 3.4 billion tons annually [11]. Inefficient waste management practices in many developing nations such as indiscriminate dumping, open burning, and unregulated landfilling continue to harm ecosystems. Plastics and glass, in particular, are major contributors to pollution. Approximately 115.6 million metric tons of plastic waste, largely PET, are produced annually [12]. Although PET is the most recycled plastic, only 20% is effectively recovered, while the rest accumulates in landfills or the environment. Likewise, only 27.1% of glass waste is recycled, mainly due to high processing costs [9].

In construction, gypsum (the base material of plaster of Paris, POP) is valued for being lightweight and fire-resistant, but its brittleness and low strength limit structural applications [12, 13]. To address these limitations, reinforcing fibers have been explored, significantly improving mechanical performance [14]. Waste PET has proven particularly useful in composite manufacturing due to its strength, toughness, and recyclability [15]. Studies show that PET enhances the durability, tensile strength, and water resistance of cementitious materials [17], and when incorporated into gypsum composites, it improves compressive and flexural strength while reducing brittleness [16, 18]. Similarly, glass fibers are widely recognized for their high tensile strength, corrosion resistance, and low density [19]. Their inclusion in gypsum composites improves flexural and compressive strength, reduces cracking, and increases impact resistance [20, 21].

In recent years, research on the development and application of composite panels has expanded significantly, largely due to their superior properties compared to individual components [22].

Previous studies have demonstrated that composite boards made from sawdust or wood dust can be effectively applied as wall partitions and ceiling materials in construction [23]. Similarly, rice husk-based composites have been developed for use as ceilings by Guna *et al.*, [24], partition panels Damanhur *et al.*, [25], aircraft components, and furniture. Other natural fibers such as coconut husks by Roberto et al., [22], rattan, melon seed husks, and tiger nut fibers by Ugochukwu *et al.*, [26] have also been incorporated into composites with promising results.

Nepal *et al.* [5] investigated the reinforcement of plaster of Paris (POP) using kenaf bast fibers, which were retted and chemically modified through a Control System Tank Retting (CSTR) process and treated with sodium lauryl sulfate. In another study, Roberto *et al.*, [22] reinforced POP with paper pulp to reduce weight and improve issues such as crack propagation and poor flexural strength. Nepal et al. [5] also examined POP reinforced with different particle sizes (38, 75, and 150 μm) and varying percentages of E-type glass fibers, using locally sourced POP from Ogun State as the matrix.

Technological advances in glass fiber recycling have also been notable. Barnett [27], developed processes to virtually eliminate glass fiber production waste by converting it into commercially viable products, potentially preventing the landfilling of about 250,000 tons annually. Further, Nepal *et al.*, [5] explored the influence of glass fiber length and content on the flexural, tensile, and impact properties of water-resistant gypsum binders. Their findings revealed that 4–9% glass fibers of 50 mm length provided optimal strength improvements, while immersion tests showed enhanced water resistance compared to plain plaster composites.

The durability of PET fiber reinforcements has also been studied. Silva *et al.*, [18], investigated cement-based mortars containing PET fibers, analyzing their compressive, tensile, and flexural strengths, as well as modulus of elasticity and toughness over 164 days. Although PET did not significantly improve strength or stiffness, toughness declined due to fiber degradation from alkaline hydrolysis, as confirmed by FTIR (Fourier Transform Infrared spectroscopy) and SEM (Scanning Electron Microscopy).

Other approaches have focused on functional modifications of gypsum composites. Sari *et al.*, [28], developed composite phase change materials (PCMs) by combining organic PCMs with building materials to create stable composites for thermal energy storage in heating,

ventilation, and air conditioning systems. Similarly, Khalil *et al.*, [29] studied modified gypsum plaster reinforced with sand, silica fume, silica gel, rice husk, slag, calcium carbonate, or polyvinyl acetate (PVA). Using FTIR, XRD, and SEM analyses, they found that these additives altered the crystal morphology of set plaster, improving both compressive strength and water resistance. Additionally, Sair [30], evaluated gypsum composites reinforced with cork and cardboard waste fibers. Tests of their thermal, hygrometric, mechanical, and acoustic properties demonstrated that such eco-friendly composites are well-suited for diverse construction applications.

According to the literature only little is known about the morphological properties of plaster of Paris / waste polyethylene terephthalate - glass fiber composite. The aim of this research is to produce POP with 5 to 15 g substitution of PET and waste glass from the gypsum and check its effect on the properties of the composites and also to carryout morphological analysis using SEM and FTIR.

MATERIALS AND METHOD

Sample Collection

Raw Gypsum was obtained from Ashaka, Gombe State, Nigeria and ground in the factory. The PET used for this research is the common bottled water PET that was obtained from Kashere landfills near the bridge linking Kashere to Billiri, Gombe State, Nigeria. Glass fiber for this research was obtained from Alkaleri in Bauchi State, Nigeria.

Sample Preparation

Raw gypsum was first ground in a steel ball mill for 2 minutes, then calcined at 180 °C for 3 hours and subsequently aged in air for 2 days to obtain Plaster of Paris. The POP was blended with varying proportions of glass fiber and PET based on the formulation in Table 1. Waste PET, sourced from Kashere, was cut into small pieces (about 20 mm) using scissor and thoroughly washed with distilled water. Glass fibers were similarly cleaned and reduced to sizes of approximately 10 mm using a mortar and pestle. For the control sample, the gypsum powder was mixed with water in a beaker to form a paste, which was poured into a mold, with fibers strategically inserted to act as reinforcement rods. Other composite samples were prepared by partially substituting the gypsum with PET and glass fibers in the specified proportions outlined in Table 1.

Composition Formulation

Due to the absence of universal method for the formulation of plaster-based compositions, the research developed a consistency table for trials. Table 1 shows the formulation used.

Table 1: Formulation used in making the various matrix/fillers

SAMPLE	GYPSUM (g)	STRAW (g)	W/G (g)	PET (g)	Glass (g)
A	100	1	0.5	0	0
B	95	1	0.5	5	0
C	95	1	0.5	0	5
D	90	1	0.5	0	10
E	90	1	0.5	10	0
F	90	1	0.5	5	5
G	85	1	0.5	10	5
H	85	1	0.5	5	10

Compounding

The gypsum powder is mixed with the amount of water in a beaker and then poured into the mold. It is allowed to set and harden equally, the amount PET and glass are varied from the amount of gypsum powder based on the formulation ratio. The required volume of distilled water is poured onto the mixture and then remixed by stirrer for 5 minutes. The mixture is poured in a mold of the standard shapes for further analysis. After 30 minutes, the sample is removed from the mold and dried in sun at approximately 3 days [31].

Pressing into shapes

The mixed samples after compounding, is immediately pressed into the mold of rectangular and dog-bone shapes.

Morphological Analysis and FTIR

To evaluate the morphology of the composites, a sample resulting from the Flexural test is subjected to SEM (EVO Series). FTIR analysis on the hardened samples is used to check the functional groups due to the compounding [32].

RESULTS AND DISCUSSION

Scanning Electron Microscopy Analysis

The SEM analysis provided an understanding of the microstructural behavior of the gypsum composites reinforced with PET and waste glass fibers. The SEM images showed that both PET and glass fibers were uniformly dispersed within the gypsum (POP) matrix at lower fiber loading levels, which is a critical factor in ensuring effective stress transfer and mechanical integrity. The good dispersion suggests strong interfacial adhesion between the matrix and the reinforcement materials, which facilitates efficient load distribution under mechanical stress. This supports the enhanced tensile and flexural strength observed in the mechanical tests and aligns with the findings of Zhou *et al*. [33], who reported that uniform fiber distribution improves composite strength by minimizing stress concentrations. However, at higher reinforcement loadings, SEM images revealed fiber agglomeration clusters of PET or glass fibers that disrupt the homogeneity of the matrix. These agglomerates can create localized stress points and voids, which act as initiation sites for cracks under load, potentially reducing the composite's mechanical performance. This phenomenon is consistent with the observations of Malik *et al*., [34], who noted that excessive fiber content leads to poor wetting and reduced bonding between fibers and the matrix, resulting in inhomogeneous composites.

In addition, the micrographs revealed a significant reduction in porosity in PET and glass fiber-reinforced samples compared to the control (pure gypsum). This densification is particularly important, as lower porosity correlates with reduced water absorption, enhanced durability, and improved dimensional stability key factors for materials exposed to humid or wet environments. Chowdhury *et al*. [35] also noted that polymer-reinforced composites exhibit lower porosity due to the filling effect of fibers and improved packing density, which helps explain the reduction in water uptake and decreased density observed in the experimental results.

Furthermore, SEM analysis showed that the PET fibers, due to their thermoplastic nature and surface smoothness, formed good contact with the gypsum particles, promoting mechanical interlocking and adhesion. Similarly, the rigid and angular nature of the glass particles created a barrier-like network within the matrix, contributing to structural stiffness and reduced permeability. These microstructural attributes are in line with the findings of Rahman *et al*., [36], who demonstrated that the inclusion of PET and glass in gypsum matrices leads to more compact

structures and stronger fiber-matrix bonding. Figure 1 shows SEM analysis of Sample A (pure gypsum).

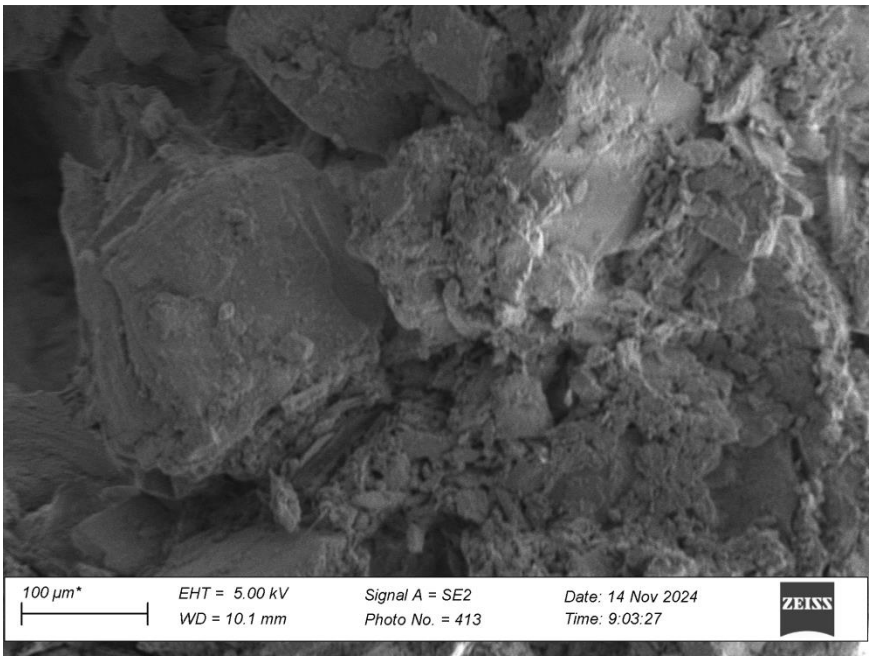

Figure 1: Sample A image from the SEM

The SEM micrograph of Sample A revealed a coarse and irregular surface morphology dominated by angular, plate-like crystalline particles, with heterogeneous sizes and random orientation. This observation is characteristic of gypsum's inherent brittleness and crystalline structure, which tends to fracture along defined crystallographic planes rather than undergo plastic deformation under stress. These features are consistent with findings by Singh and Garg [20], who observed similar morphologies in unreinforced gypsum, attributing the behavior to its low fracture toughness and microstructural irregularity.

The microstructure also displayed interparticle voids and high porosity, indicating a loosely packed granular arrangement, which is typical of materials with limited mechanical integrity. High porosity can lead to increased capillary action and water absorption, significantly affecting dimensional stability and durability in moisture-exposed environments. This aligns with the work of Liu *et al*. [21] who highlighted that porous gypsum materials exhibit poor mechanical strength and high water retention capacity, making them susceptible to long-term degradation, especially when used in humid climates or as building materials.

A feature in the SEM images is the layered appearance and sheet-like particle stacking, which may reflect the presence of multiple gypsum phases, such as calcium sulfate dihydrate ($CaSO_4 \cdot 2H_2O$) and hemihydrate ($CaSO_4 \cdot 0.5H_2O$). The coexistence of these phases could result from partial dehydration during processing or incomplete crystallization. According to Zhang et al. [16] the mineralogical composition of gypsum significantly affects its hydration kinetics, setting time, and mechanical strength, particularly when used in composite formulations. Moreover, such layering without uniform packing suggests structural inhomogeneity, which can impair load transfer and reduce compressive and tensile strength, as reported by Mohammad *et al*. [37].

Additionally, the lack of any visible fiber reinforcement or compact filler network in Sample A confirms its role as the control, unmodified matrix. Its rough morphology, random crystalline orientation, and pronounced porosity explain the poor performance in mechanical tests such as tensile, flexural, and water absorption. Compared to the reinforced samples, the pure gypsum matrix lacks any mechanism to bridge microcracks or redistribute stress, hence its lower mechanical performance and greater susceptibility to brittle fracture. As described by Chowdhury *et al.,* [35] introducing polymeric or fibrous reinforcements into gypsum matrices substantially alters their microstructure by filling pores and enabling better stress transfer, which is not evident in this control sample.

Fig 2 shows the SEM analysis of the gypsum–PET composite (95 g gypsum + 5 g PET).

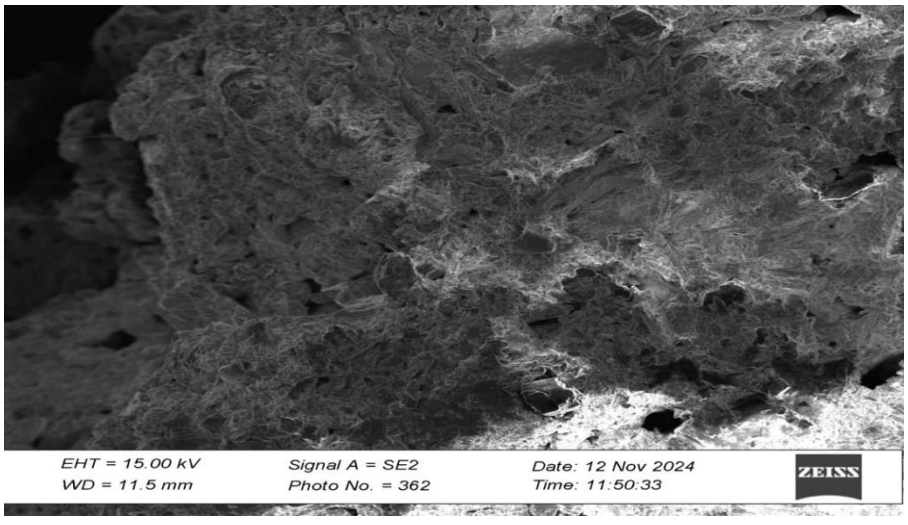

Figure 2: Image of Sample B

It revealed a heterogeneous and irregular surface morphology, marked by angular gypsum particles embedded within a matrix containing PET fragments. The plate-like, crystalline appearance of gypsum was preserved, indicative of its inherent brittleness and cleavage along specific crystallographic planes, a behavior well-documented by Singh & Garg [20]. Interspersed between these particles were visible voids and interparticle spaces, suggesting a porous structure that can influence the material's mechanical and moisture-absorbing properties.

Whereas PET was introduced to improve ductility, its partial or non-uniform dispersion could be observed in some regions, hinting at incomplete interfacial bonding with the gypsum matrix. This phenomenon has been widely reported in polymer–ceramic composites, where poor compatibility between phases results in microstructural discontinuities, negatively affecting load transfer and homogeneity [16]. The resulting porosity and layered morphology may also stem from differential shrinkage or incompatibility in thermal expansion between PET and gypsum during setting or curing, which has been shown to cause micro-cracking or weak interfaces [37, 38].

The layered structure seen in the image could indicate phase separation or incomplete matrix integration, especially since PET is hydrophobic, while gypsum is hydrophilic. This mismatch can hinder molecular-level adhesion, a critical factor for achieving a uniform composite. Studies such as Arefi and Rezaei-Zarchi [46] have demonstrated that modifying the polymer surface (e.g., through compatibilizers or coupling agents) is often necessary to enhance bonding in such systems.

Despite these structural limitations, the inclusion of PET still confers certain advantages. PET’s flexibility and toughness may act to bridge microcracks or provide energy dissipation zones, improving the composite’s resistance to sudden fracture under tensile or impact loads [35]. However, this benefit is contingent upon adequate dispersion and adhesion of the polymer phase factors that appear to be suboptimal in this composite formulation.

Fig 3 is the SEM analysis result for Sample C.

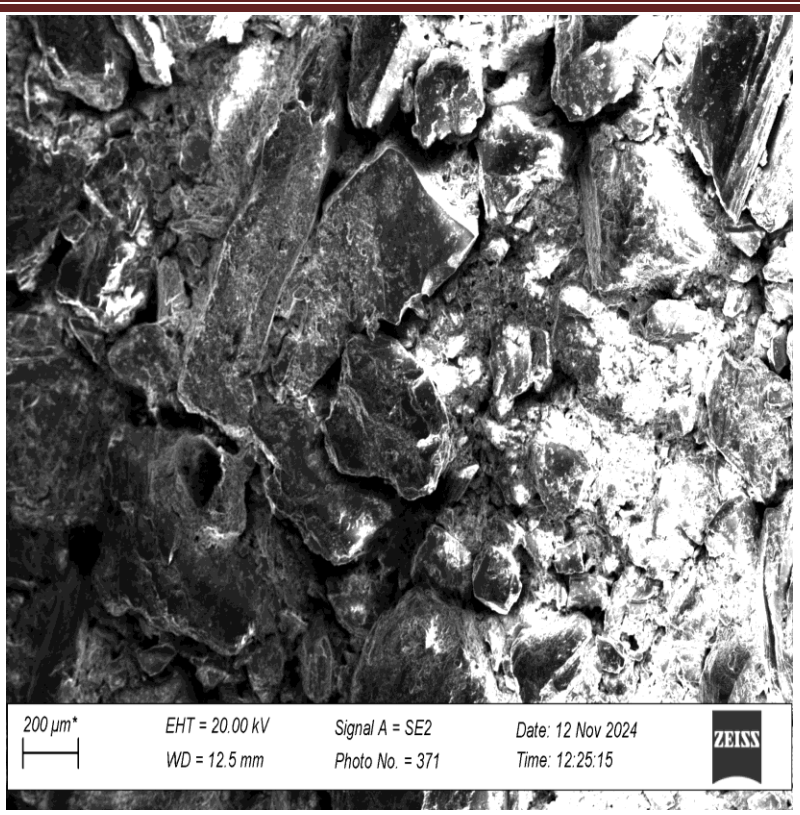

Figure 3: Image of Sample C

It displays a rough and irregular surface topology, with prominent angular, crystalline particles of varying sizes, arranged in a non-uniform pattern. These features are indicative of a brittle fracture mechanism common in crystalline solids like gypsum. The sharp-edged morphology suggests that the material breaks along cleavage planes rather than deforming plastically, aligning with the mechanical characteristics of mineral-based composites described by Singh & Garg [20]. Such morphology also implies anisotropic stress distribution, which can negatively affect toughness and crack resistance unless modified by suitable reinforcements.

The presence of visible intergranular voids further confirms that the composite exhibits moderate porosity, which can be both beneficial and detrimental depending on the intended application. High porosity increases the material's water absorption capacity and thermal insulation but may reduce mechanical strength and density. This observation aligns with the findings of Liu *et al*. [21] who reported that gypsum-based composites with higher porosity showed improved insulation but lower load-bearing performance. In construction applications, this trade-off must be managed carefully to balance strength and durability.

The micrograph also suggests a heterogeneous distribution of phases, likely due to incomplete mixing or incompatibility between gypsum and the Plastic particles. Although waste PET is hard, its plastering nature contrasts with the crystalline gypsum matrix, possibly resulting in poor interfacial bonding. As Zhang et al., [16] observed, such heterogeneity can lead to localized stress concentrations and compromise mechanical performance unless surface modification or compatibility strategies are employed.

Fig 4 shows the SEM analysis result for the gypsum-glass (D) composite sample.

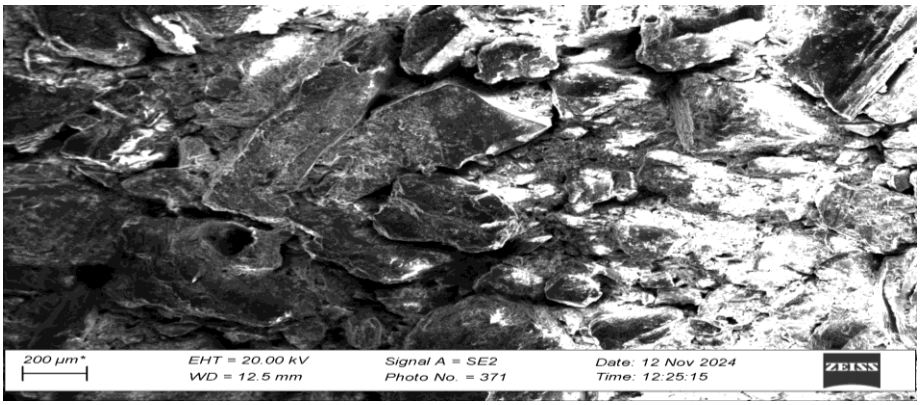

Figure 4: Image of Sample D

The SEM micrograph reveals a rough, jagged surface topology with plate-like, angular particles that vary significantly in size and orientation. These features are typical of brittle and crystalline materials, including gypsum and certain forms of glass. As described by Singh and Garg [20] such particles tend to fracture along cleavage planes due to their crystalline nature, exhibiting limited plastic deformation. The microstructural heterogeneity and irregular texture further suggest that the composite matrix lacks a well-integrated particle arrangement, which can negatively affect stress transfer, mechanical cohesion, and fracture resistance.

The presence of visible interparticle voids in the SEM images confirms a porous and loosely packed structure, which plays a critical role in determining the composite's mechanical integrity, water resistance, and thermal stability. In gypsum-based materials, porosity often arises from the crystalline nature of the particles, air entrapment during mixing, and interfacial gaps created by particle incompatibility. As noted by Liu *et al.*, [21], such porosity not only reduces mechanical strength but also increases water uptake, making the material more vulnerable in humid or aquatic environments.

The inclusion of glass particles, which are amorphous, hard, and chemically inert, appears to contribute significantly to this microstructural porosity. The difference in surface chemistry and thermal expansion coefficients between glass and gypsum can lead to poor interfacial bonding, creating weak zones within the matrix. These mismatched properties often result in the formation of interfacial microcracks or debonded regions, especially during setting or drying processes. According to Zhang *et al*. [16] this mismatch between reinforcement and matrix leads to phase separation and uneven stress distribution, especially under mechanical loading or thermal cycling.

The observed layered structure and localized phase discontinuities are suggestive of microstructural inhomogeneity, possibly caused by inadequate dispersion or incompatibility during mixing. Gypsum, being a hydrophilic and hydrated mineral ($CaSO_4 \cdot 2H_2O$), tends to bind water and forms a crystalline network, while glass, composed primarily of SiO_2, remains amorphous and hydrophobic. The combination of these contrasting materials without proper compatibilization may result in phase separation during the curing process. As observed by Mohammad *et al*., [37] and Vola *et al*., [44], such phase boundaries often manifest as microvoids or microcracks, especially if the two components undergo different volumetric changes upon setting or drying.

Although glass particles can improve compressive strength and rigidity due to their hardness, their brittle nature and poor adhesion to the gypsum matrix may compromise tensile and flexural strength, particularly if the glass content exceeds the optimal loading threshold. This is consistent with the findings of Rahman *et al*., [36], who demonstrated that excessive incorporation of hard fillers in gypsum can lead to stress concentration sites, reducing overall material toughness and energy absorption capacity under load.

Fig 5 shows the SEM of Sample E.

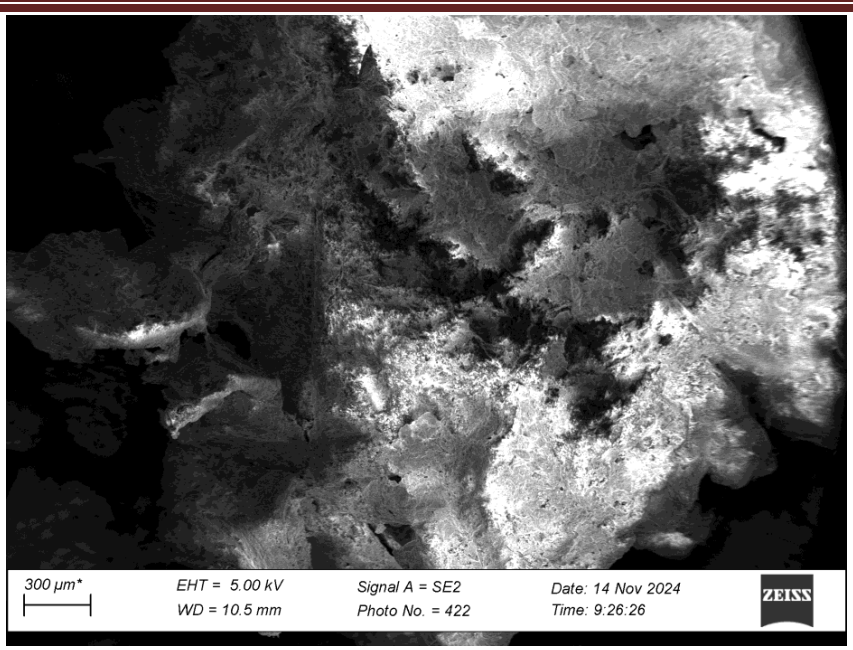

Figure 5: Image of Sample E

The analysis shows SEM micrograph of the gypsum-PET composite. It reveals a rough, uneven surface morphology, characterized by angular, plate-like particles and random spatial orientation. These features are characteristic of crystalline gypsum, which tends to fracture along cleavage planes, leading to sharp and irregular geometries. Such morphology contributes to brittle behavior, particularly under compressive and flexural loading, as confirmed by Singh & Garg [20]. The irregularity in particle shape and size may also suggest that the material has undergone mechanical fragmentation or inadequate processing, which could lead to structural inconsistencies within the matrix.

Visible interparticle voids and porosity were also observed, suggesting that the material has a heterogeneous and non-densely packed structure. In gypsum-based composites, porosity arises due to several factors, including air entrapment during mixing, incomplete hydration, or weak interfacial bonding between gypsum and additives. As stated by Liu *et al*., [21], elevated porosity in gypsum composites is often linked to increased water absorption, but it also reduces compressive strength and stiffness. This poses challenges for durability, especially in moisture-prone environments or structural applications.

The non-uniform distribution of particles in the matrix further suggests ineffective mixing or phase separation between the gypsum and PET phases. The PET, being a hydrophobic thermoplastic, may not integrate seamlessly with the hydrophilic gypsum matrix, leading to

phase incompatibility and microstructural inhomogeneities. According to Zhang et al., [16], this mismatch can result in interfacial debonding, microcrackformation, and compromised mechanical performance if not properly addressed through surface modification or compatible use.

The layered appearance in the SEM image could also indicate incomplete matrix integration or the presence of distinct gypsum and polymeric phases. PET, known for its toughness and ductility, may offer localized energy dissipation and flexibility under load, but without good interfacial adhesion, its reinforcing effect remains limited. This is supported by Mohammad *et al*., [37], who emphasized that the thermomechanical mismatch between polymers and mineral matrices often causes internal stress accumulation, particularly under thermal cycling or prolonged use. Moreover, studies by Mansour *et al*. [38] have shown that PET-modified gypsum composites require compatibility enhancement, such as through chemical grafting or the use of coupling agents, to improve interfacial adhesion and dispersion.

Despite these structural limitations, the inclusion of PET has the potential to reduce brittleness and improve impact resistance or toughness. However, the random dispersion and agglomeration of PET particles, as inferred from the SEM morphology, indicate that the current composite formulation may need optimization. Chowdhury *et al*. [35] argue that uniform distribution of polymeric phases within mineral matrices is crucial for balanced mechanical properties, and poor dispersion can create stress concentration zones that serve as crack initiation points under mechanical loads.

Fig 6 shows the SEM imaging sample F.

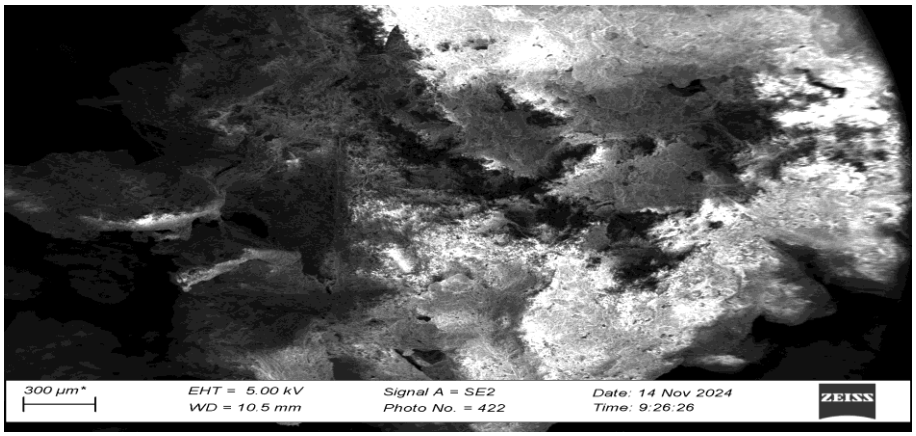

Figure 6: Image of Sample F

The SEM micrograph reveals a heterogeneous surface texture characterized by sharp-edged, angular, and plate-like particles, varying widely in size and orientation. These characteristics are consistent with the crystalline and brittle nature of gypsum, which tends to cleave along specific crystallographic planes under stress, producing irregular fracture patterns [20]. This morphology contributes to its low toughness and poor resistance to crack propagation. The absence of round or ductile features further confirms the inherent brittleness of the matrix, limiting its application in load-bearing or high-impact environments unless reinforced with polymeric or fibrous additives.

The presence of interparticle voids and gaps in the microstructure indicates significant porosity, which can arise from incomplete packing, air entrapment, or volume shrinkage during the hydration and setting process of gypsum. According to Liu *et al*., [21], porosity plays a dual role: it improves water retention capacity, which is favorable for applications like plastering and horticultural soil conditioners, but compromises mechanical integrity, especially under compressive or flexural stress. Moreover, high porosity can accelerate deterioration in humid environments due to capillary water transport, increasing the risk of microcrack propagation and matrix degradation [39].

The layered appearance and microstructural stratification observed in the SEM image further suggest phase separation or differential distribution of components in the composite system. This could be attributed to incomplete mixing, incompatibility of constituent phases, or differences in crystallization kinetics, particularly between the gypsum matrix and reinforcing agents like polyethylene terephthalate (PET), glass particles, or other polymeric fillers. These phases may not exhibit ideal chemical or physical affinity, leading to weak interfacial bonding. As noted by Mohammad *et al*., [37], mismatches in thermal expansion coefficients or surface energy between mineral and polymer phases can result in microstructural inhomogeneities, which compromise load transfer efficiency across the matrix-filler interface.

In addition, the anisotropic distribution of layered domains may reflect directional solidification patterns, sedimentation during casting, or inconsistent polymer dispersion, especially if the composite was not thoroughly blended prior to setting. According to Rahman *et al*., [36], such inconsistencies result in localized stress concentrations during mechanical loading, promoting crack initiation and delamination between phases. Moreover, this stratification can contribute to moisture pathways, further weakening the structural integrity over time.

It is also important to consider the influence of the reinforcing additives on the microstructure. For instance, glass particles, while improving stiffness and dimensional stability, may exacerbate brittle behavior if not well integrated, especially without coupling agents. PET additives, on the other hand, can introduce toughening mechanisms such as crack deflection or energy dissipation, but only if they are well-dispersed and adhesively bonded to the mineral matrix [35]. Inadequate interfacial adhesion leads to debonding under stress, acting as a flaw rather than reinforcement.

Fig 7 shows the SEM image of sample G.

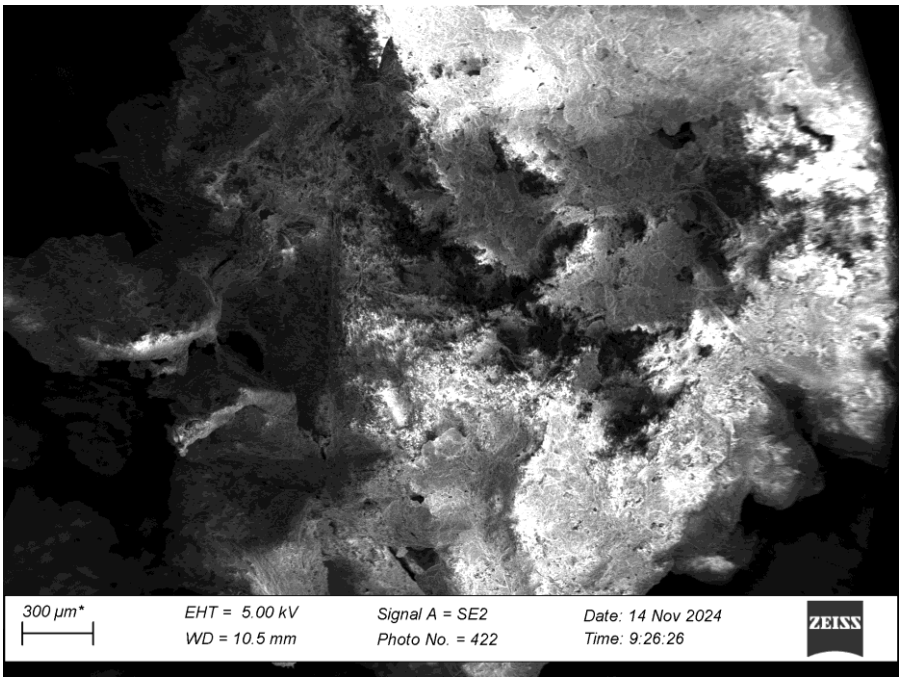

Figure 7: Image of Sample G

The SEM micrograph presents a rough and irregular surface morphology, characterized by angular, plate-like particles of varying sizes and a random arrangement. These morphological features suggest that the material exhibits brittle and crystalline properties, which are typical of gypsum-based and mineral composites [20]. The angular structure of the particles indicates that the material is likely to undergo brittle fracture rather than ductile deformation, a common behavior in crystalline solids.

The visible interparticle spaces in the micrograph suggest that the sample has a porous and heterogeneous structure, which could significantly influence mechanical properties, water absorption, and durability. High porosity in gypsum materials, as noted by Liu *et al.*, [21], can increase water retention, which is beneficial for hydration and setting reactions but may also

contribute to reduced mechanical strength. The heterogeneous nature of the sample indicates the potential for variations in phase composition, possibly due to processing conditions, impurities, or additives [16].

The layered appearance observed in the SEM micrograph suggests a complex material composition, possibly resulting from phase separation or incomplete material integration. The composite materials, glass and polymers, are present and they interact differently with the gypsum matrix, leading to microstructural in homogeneities [37]. This could influence the mechanical performance of the material.

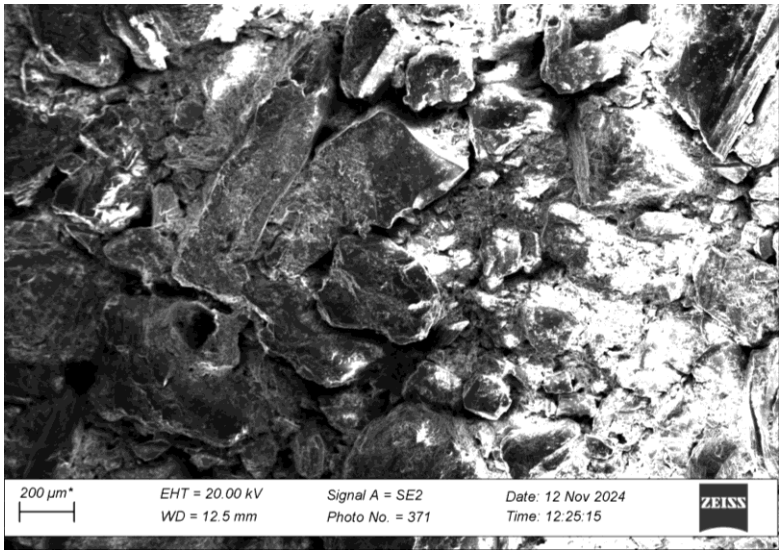

Figure 8: Image of Sample H

Fig 8 shows the SEM micrograph of sample H and reveals a rough and irregular surface morphology, consisting of angular, plate-like particles of varying sizes and a random arrangement. This morphology suggests that the material exhibits brittle and crystalline characteristics, which are commonly associated with gypsum-based materials and other mineral composites [20]. The angular shape of the particles implies that the material undergoes brittle fracture, meaning it breaks along distinct planes rather than deforming plastically. This characteristic is typical of crystalline materials where atomic bonding favors cleavage along certain crystallographic planes.

The presence of visible interparticle spaces suggests that the sample has a porous and heterogeneous structure, which can significantly affect its mechanical strength, durability, and water absorption capacity. High porosity in gypsum materials, as highlighted by Liu *et al.*, [21],

often leads to increased water retention, which can be beneficial for hydration and setting reactions. However, excessive porosity can also result in lower mechanical strength, as the voids can act as stress concentrators that weaken the overall structure. Additionally, the heterogeneous nature of the sample indicates the potential for variation in phase distribution, which could arise due to differences in crystallization, impurities, or the presence of secondary phases [16].

The layered appearance in the SEM image suggests a complex material composition, possibly due to phase separation or differential adhesion between material phases. The sample includes additional components, such as polymeric, glass and fibrous reinforcements, these materials interact differently with the gypsum matrix, leading to structural inconsistencies or weak interfacial bonding [37]. The presence of layering could also indicate variations in crystallization rates or mechanical processing effects, influencing the final material properties.

Fourier Transform Infrared Radiation

Figure 9 shows the FTIR spectrum of Sample A.

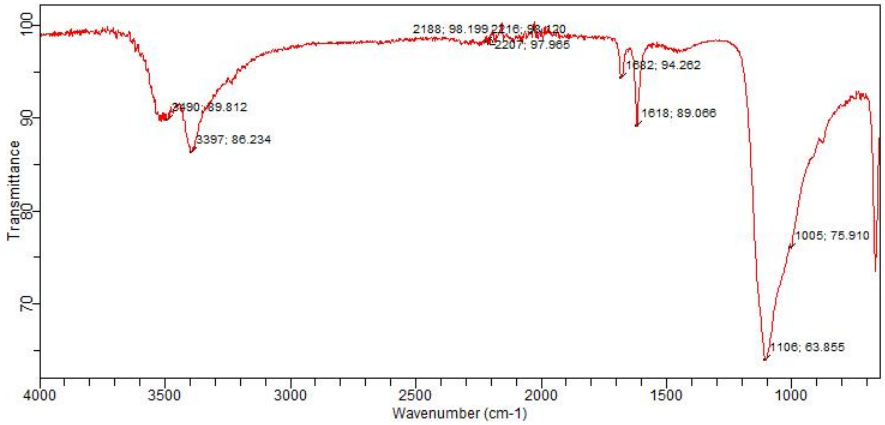

Figure 9: Spectrum of Sample A

It confirms its identity as pure gypsum ($CaSO_4 \cdot 2H_2O$) through the presence of characteristic absorption bands corresponding to its molecular structure. The broad and intense H-O–H stretching vibration peak at around 1618 cm^{-1} is indicative of the hydroxyl groups from the water of crystallization, confirming that the gypsum is in its dihydrate form ($CaSO_4 \cdot 2H_2O$). This broad peak typically arises due to hydrogen bonding among water molecules within the gypsum crystal lattice, a feature consistently reported in gypsum mineral studies [40].

The sulfate ion (SO_4^{2-}) in gypsum shows distinct and strong absorption peaks due to its symmetric and asymmetric vibrational modes. The absorption bands observed at 1005 cm^{-1} and

1005 cm^{-1} correspond to the ν_3 asymmetric stretching and ν_1 symmetric stretching modes of the sulfate group, respectively [41] These sulfate vibrational modes are highly sensitive indicators of the sulfate ion's environment and confirm the presence of sulfate groups as the primary anionic species in the mineral matrix. Additionally, the H–O–H bending vibration peak at approximately 1620 cm^{-1} corresponds to the bending mode of bound water molecules, further substantiating the hydrated nature of the sample [40, 41].

Beyond these primary peaks, gypsum typically shows weaker bands in the range of 600–700 cm^{-1} associated with sulfate bending vibrations (ν_2 and ν_4 modes) and lattice vibrations, which contribute to the identification of crystalline phases [41]. The FTIR spectral pattern of Sample A closely matches reference spectra of pure gypsum reported in literature, indicating minimal impurities or secondary mineral phases, such as anhydrite ($CaSO_4$) or bassanite ($CaSO_4 \cdot 0.5H_2O$), which exhibit shifts or the absence of water-related bands [41].

These spectral features are vital not only for qualitative identification but also provide insight into the degree of hydration, crystal structure integrity, and possible interactions with additives or contaminants in modified gypsum composites [42]. The presence and stability of the hydration water significantly affect the mechanical and thermal properties of gypsum, influencing its setting time, strength, and durability in construction or composite applications [40].

Figure 10 shows the FTIR spectrum of the composite containing 95 g gypsum and 5 g polyethylene terephthalate (PET).

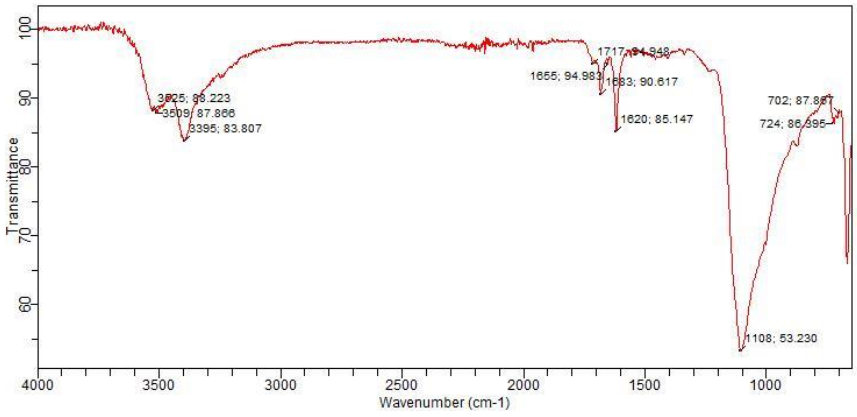

Figure 10: Spectrum of Sample B

It reveals characteristic absorption bands of both components, confirming their coexistence and partial interaction within the matrix. The gypsum phase is identified by prominent peaks

associated with its hydrated calcium sulfate structure. Specifically, the O–H stretching vibrations appear as broad bands around 3295 cm^{-1} and 3259 cm^{-1}, which correspond to the hydroxyl groups in the water of crystallization and hydrogen-bonded water molecules within the gypsum lattice [40].

The H–O–H bending modes are observed at approximately 1655 cm^{-1} and 1620 cm^{-1}, indicating bound water molecules that play a key role in gypsum's hydration state and mechanical properties [41]. Additionally, sulfate ion stretching vibrations manifest at 1108 cm^{-1}, with accompanying bending modes near 724 cm^{-1} and 702 cm^{-1}, confirming the persistence of the sulfate tetrahedra within the gypsum structure [41].

The spectrum also exhibits several characteristic peaks attributable to PET, albeit some of these overlap partially with the gypsum absorption bands due to their proximity in spectral regions. Notably, weak C–H stretching vibrations appear in the range of 3100–2800 cm^{-1}, which are typical of the aliphatic and aromatic C–H bonds present in PET's molecular backbone [45]. The strong ester carbonyl (C=O) stretching vibration near 1717 cm^{-1} is a definitive signature of PET's ester linkage, which is responsible for its rigidity and thermal stability (Sabatini *et al*., 2019). Furthermore, C–O stretching vibrations are evident between 1240–1100 cm^{-1}, although these bands partially overlap with the sulfate region of gypsum, complicating distinct peak assignment [41, 45].

The partial overlap of PET's C–O stretching with gypsum's sulfate absorption peaks suggests potential interfacial interactions or physical blending within the composite, though the degree of chemical bonding or compatibility may be limited due to the inherent hydrophobicity of PET and hydrophilicity of gypsum [37]. Such overlapping peaks are common in polymer-mineral composites and indicate that while PET is physically embedded, strong chemical bonding might require further surface modification or compatibilization [35].

The retention of sharp and distinct gypsum hydration bands alongside PET ester and hydrocarbon peaks highlights that the composite preserves the individual structural integrity of both constituents, which is essential for maintaining their complementary mechanical properties. Gypsum provides stiffness and compressive strength, while PET contributes ductility and toughness, making this composite potentially advantageous for applications requiring a balance of rigidity and flexibility [36].

The FTIR analysis confirms the successful incorporation of PET into the gypsum matrix, with identifiable spectral features of both materials and partial spectral overlap indicating interfacial co-existence but limited chemical interaction without specific coupling agents.

Figure 11 shows the FTIR spectrum of the gypsum composite clearly confirms the presence of gypsum through several characteristic absorption bands.

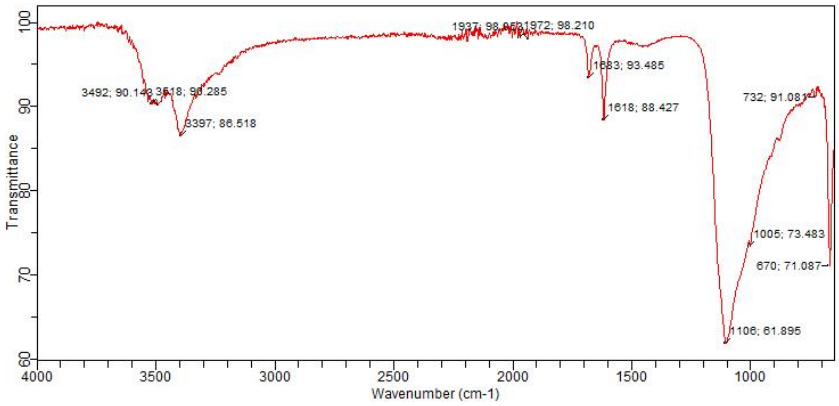

Figure 11: Spectrum of Sample C

The broad O–H stretching vibrations observed near 3625 cm^{-1} and 3399 cm^{-1} correspond to the hydroxyl groups and structural water molecules in the dihydrate form of gypsum ($CaSO_4 \cdot 2H_2O$), consistent with hydrogen bonding within the crystal lattice [40, 41]. The prominent H–O–H bending vibration at approximately 1620 cm^{-1} further corroborates the presence of bound water, which is essential for the hydration state and mechanical behavior of gypsum [41].

Sulphate ions, fundamental to gypsum's structure, exhibit characteristic stretching vibrations centered around 1106 cm^{-1}, which are linked to the asymmetric stretching modes of the sulfate tetrahedron (SO_4^{2-}) [41]. Additionally, the distinct peak at about 883 cm^{-1} is often assigned to bending vibrations within the gypsum lattice, reinforcing the identification of the mineral phase [20].

The additional absorption band at approximately 1005 cm^{-1} is indicative of silica (Si–O) stretching vibrations, revealing the presence of silicate species originating from the incorporated glass component in the composite. Silica-based glasses typically display strong Si–O–Si asymmetric and symmetric stretching bands in the 1000–1100 cm^{-1} region [15, 43]. The overlap between the sulfate ν_3 stretching modes and silicate vibrations in this spectral range suggests that the composite features both gypsum and glass phases interspersed at the molecular level.

Such spectral overlapping is typical in composites containing mineral and silicate phases, and it confirms the successful integration of waste glass particles into the gypsum matrix. This integration can lead to enhanced mechanical properties and durability due to the combined effects of gypsum's crystalline rigidity and glass's hardness and chemical stability [36]. The presence of silicate bands may also imply some degree of interaction or bonding between the gypsum and glass phases, which can influence the composite's microstructure and overall performance [16].

The overlapping region between 1000 and 1100 cm^{-1} serves as a diagnostic spectral window to monitor the relative proportions and interaction of sulphate and silicate groups in composite materials. Careful deconvolution of these peaks can provide insights into phase distribution, degree of mixing, and potential chemical modifications occurring during composite fabrication [41].

Figure 12 shows the FTIR spectrum of the composite containing 90 g gypsum and 10 g glass exhibits distinct vibrational bands characteristic of both gypsum and silicate glass components, confirming the successful incorporation of glass into the gypsum matrix.

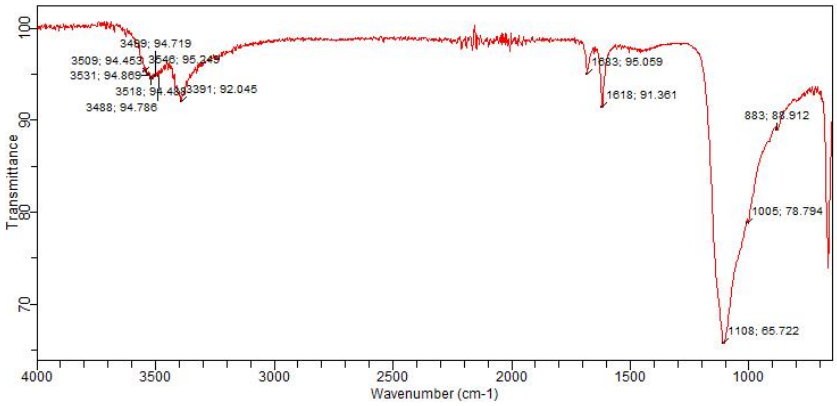

Figure 12: Spectrum of Sample D

The gypsum phase is identified by multiple O–H stretching peaks located around 3498 cm^{-1}, 3509 cm^{-1}, 3518 cm^{-1}, and 3631 cm^{-1}, which correspond to hydroxyl groups involved in hydrogen bonding and water molecules bound within the gypsum crystalline structure [40, 41]. These multiple bands suggest variations in hydrogen bonding environments within the dihydrate gypsum phase ($CaSO_4 \cdot 2H_2O$), reflecting the complexity of its hydrated lattice.

The H–O–H bending vibration near 1618 cm^{-1} further confirms the presence of structural water, a key feature influencing gypsum's setting behavior and mechanical properties [41]. Sulfate ions (SO_4^{2-}) present in gypsum are represented by strong stretching vibrations observed at 1108 cm^{-1} and 1005 cm^{-1}, consistent with the asymmetric and symmetric stretching modes of sulfate tetrahedra [20, 41].

In addition to the gypsum-related peaks, the presence of the glass phase is clearly indicated by broad and overlapping absorption bands attributed to silicate structures. The Si–O–Si asymmetric stretching vibrations are detected in the 1200–900 cm^{-1} range, overlapping partially with gypsum sulfate stretching bands [15, 43]. These peaks arise from the amorphous silica network in glass, where the silicon–oxygen bonds form the backbone of the glass matrix. Furthermore, the Si–O bending vibrations, observed within the 500–800 cm^{-1}region, provide additional confirmation of the silicate glass component [43].

The overlapping of sulfate and silicate bands in the 900–1200 cm^{-1} spectral window is a common feature in gypsum-glass composites, reflecting the coexistence and possible interfacial interactions between the crystalline gypsum and amorphous glass phases [16]. This spectral overlap may indicate some degree of physical intermingling or chemical interaction at the composite interface, potentially affecting properties such as mechanical strength, thermal stability, and water resistance [36].

The glass addition not only introduces silicate functional groups but also influences the microstructural characteristics of the composite, such as porosity and bonding between phases, which are critical for the material's durability and performance [37]. The combined FTIR signature confirms the composite's hybrid nature and suggests that the incorporation of glass may enhance certain mechanical properties by complementing the brittle gypsum phase with the harder, more chemically inert glass particles [15].

Figure 13 shows the FTIR spectrum analysis.

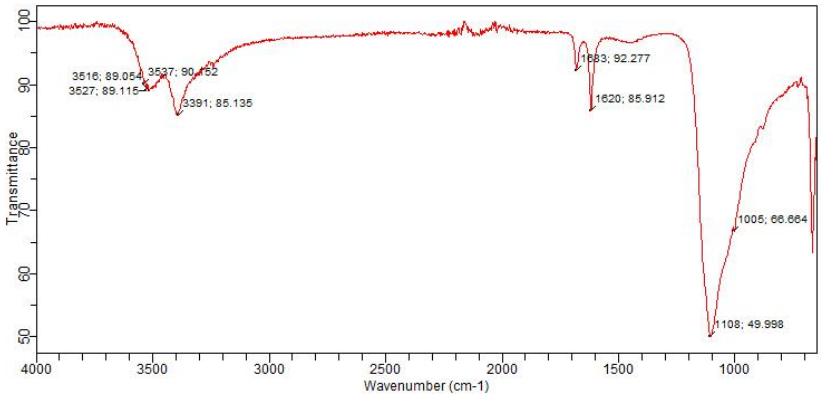

Figure 13: Spectrum of Sample E

It confirms the predominance of gypsum ($CaSO_4 \cdot 2H_2O$) in the composite through several characteristic vibrational bands. The broad O–H stretching vibrations observed around 3518 cm^{-1} and 3395 cm^{-1} are indicative of hydroxyl groups and structural water molecules, reflecting the dihydrate nature of gypsum. These peaks correspond to hydrogen-bonded water within the crystal lattice, which is critical to gypsum's physical and chemical properties [40, 41]. The H–O–H bending vibration at approximately 1618 cm^{-1} further validates the presence of molecular water within the gypsum structure, supporting its hydrated crystalline form [41].

The presence of sulfate functional groups is substantiated by the asymmetric stretching vibration of SO_4^{2-} near 1108 cm^{-1}, which arises from the vibrational modes of the sulfate tetrahedron typical of gypsum [20]. Additionally, the S–O bending vibration at around 881 cm^{-1} corroborates the identification of sulfate ions, a defining feature of the calcium sulfate mineral family [41].

Regarding the polyethylene terephthalate (PET) component, its spectral contributions are minimal but detectable. The presence of PET is indicated by weak absorption bands near 1710 cm^{-1}, corresponding to the ester carbonyl (C=O) stretching, a signature functional group in PET's molecular structure [35, 36]. Additional minor peaks near 1250 cm^{-1} and 1090 cm^{-1} correspond to C–O stretching vibrations within the ester linkages, confirming the polymer's presence despite its low concentration in the composite [34].

The absence of strong CH stretching peaks around 2900 cm^{-1}, typical of aliphatic C–H bonds, further suggests that PET's quantity in the sample is low, or that these bands are obscured by overlapping with broader O–H bands from gypsum [16]. This limited PET presence likely results in subtle modifications of the composite's properties without dominating the spectral profile.

The FTIR data indicate a composite primarily governed by gypsum's hydrated sulfate structure with minor incorporation of PET polymer. The polymer's limited spectral presence suggests it functions as a reinforcing additive, possibly enhancing flexibility or impact resistance without substantially altering the chemical composition of the matrix [35]. These findings align with previous studies demonstrating that low polymer loadings in mineral-based composites primarily affect mechanical behavior rather than chemical structure [34, 36].

Figure 14 shows the FTIR spectrum of the composite containing 90 g gypsum, 5 g PET, and 5 g glass.

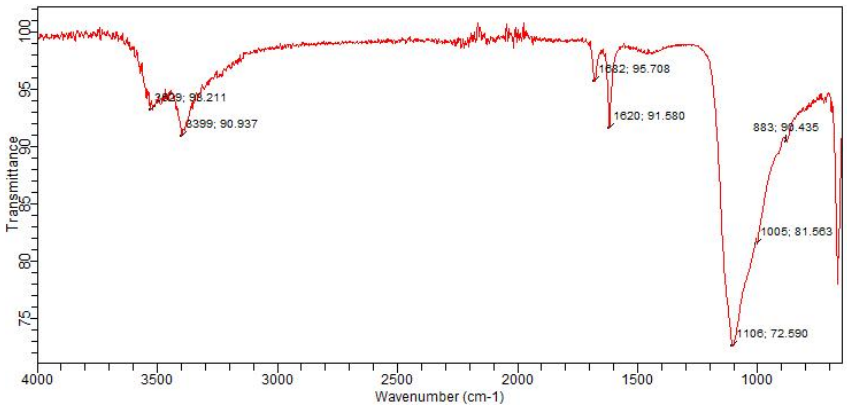

Figure 14: Spectrum of Sample F

It reveals the presence and interaction of all three components, each contributing characteristic vibrational bands. The gypsum phase is verified by the presence of strong O–H stretching vibrations observed at approximately 3624 cm^{-1} and 3490 cm^{-1}, which correspond to the hydroxyl groups involved in hydrogen bonding within the dihydrate gypsum lattice ($CaSO_4 \cdot 2H_2O$) [40, 41]. These broad O–H bands indicate structural water molecules that are integral to the gypsum crystalline structure.

The H–O–H bending vibration near 1620 cm^{-1} further confirms the bound water within gypsum, essential for its hydration and setting properties [41]. The sulfate groups manifest in the spectrum with strong asymmetric sulfate stretching around 1108 cm^{-1} and bending vibrations near 1005 cm^{-1}, both characteristic of sulfate tetrahedra within the gypsum mineral [20]. These sulfate-related absorptions are fundamental for identifying calcium sulfate minerals and relate directly to the material's mechanical and chemical behavior.

The PET component, present at 5g, is identified by distinctive C=O stretching vibrations at approximately 1715 cm^{-1}, characteristic of the ester carbonyl group, a primary functional group

in PET's polymer backbone [35, 36]. Additional C–O stretching vibrations spanning 1240–1100 cm^{-1} further confirm the presence of ester linkages within the polymer [34]. These bands may partially overlap with sulfate absorptions, but their presence underscores PET's role as a polymeric additive contributing to the composite's flexibility and impact resistance.

The glass phase, also at 5g, contributes broad absorption bands attributable to silicate structures. The Si–O–Si asymmetric stretching vibrations are evident in the 1200–900 cm^{-1} range, overlapping partially with gypsum's sulfate bands [15, 43]. Additionally, the Si–O bending vibrations in the 500–800 cm^{-1}region are typical of the silica network found in amorphous glass [43]. The overlap of silicate and sulfate bands highlights the complex nature of the composite's interfacial chemistry and microstructure, where amorphous glass phases coexist with crystalline gypsum.

This spectral overlap may indicate partial interfacial interactions or physical blending rather than chemical bonding between the gypsum matrix and glass particles, which can influence the composite's mechanical properties such as toughness and water resistance [16, 36]. The combined presence of polymer and glass fillers within the gypsum matrix creates a hybrid composite system that aims to enhance mechanical performance by leveraging the ductility of PET and the rigidity and chemical inertness of glass [37].

Figure 15 shows the FTIR spectrum of the composite with 85% gypsum, 10% polyethylene terephthalate, and 5% glass reveals distinctive vibrational bands that validate the presence and interaction of each component within the material matrix.

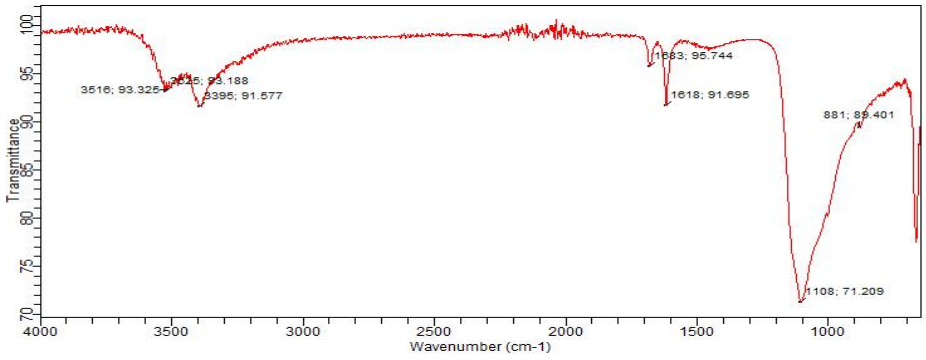

Figure 15: Spectrum of Sample G

The gypsum phase is confirmed by several characteristic absorption peaks. The O–H stretching vibration observed at around 3397 cm^{-1} corresponds to hydroxyl groups and structural water molecules inherent to the dihydrate form of gypsum ($CaSO_4 \cdot 2H_2O$), a signature feature

indicating the presence of hydrated calcium sulfate [40, 41]. The H–O–H bending vibration at approximately 1618 cm^{-1} further substantiates the existence of bound water molecules, which are critical for gypsum's crystallinity and setting properties [41].

Sulfate functional groups are distinctly observed through their stretching vibrations at 1106 cm^{-1} and 1005 cm^{-1}, corresponding to the asymmetric and symmetric stretching modes of SO_4^{2-} ions within the gypsum lattice [20]. These sulfate bands play a crucial role in determining the chemical stability and mechanical integrity of the gypsum-based matrix.

The incorporation of 10% PET is evident from several key absorptions. The strong C=O stretching band at 1718 cm^{-1} corresponds to the ester carbonyl groups present in PET's polymer backbone, a definitive marker of polyester presence [35, 36]. The aliphatic C–H stretching vibrations seen in the range of 2970–2980 cm^{-1} indicate the presence of methylene groups in the polymer chain, which contribute to PET's flexibility and ductility [34]. Additionally, the C–O stretching vibrations at 1240 cm^{-1} and 1090 cm^{-1} reflect the ether linkages within the polymer, confirming the PET's structural integrity within the composite [16].

The presence of 5% glass is substantiated by absorptions characteristic of silicate networks. The Si–O–Si asymmetric stretching vibration around 1106 cm^{-1} overlaps with the sulfate stretching region, illustrating the complex interplay between gypsum and glass components at the molecular level [43]. Moreover, the Si–O bending vibration near 800 cm^{-1} is typical of silica-based glass materials, indicating the presence of amorphous silicate phases [15]. The overlapping spectral features between gypsum sulfates and glass silicates suggest a physically blended composite where both phases coexist, potentially influencing mechanical and thermal behaviors.

The synergistic presence of PET and glass within the gypsum matrix suggests a composite designed to combine the flexibility and impact resistance imparted by PET with the rigidity and chemical stability of glass fillers. Such multi-component composites often exhibit enhanced mechanical strength, toughness, and durability compared to pure gypsum, making them suitable for applications requiring both load-bearing capacity and resistance to environmental degradation [35, 37].

Figure 16 shows the FTIR spectrum analysis of the composite samples containing gypsum, PET, and glass fibers provides clear evidence of the coexistence and interaction of these materials at the molecular level.

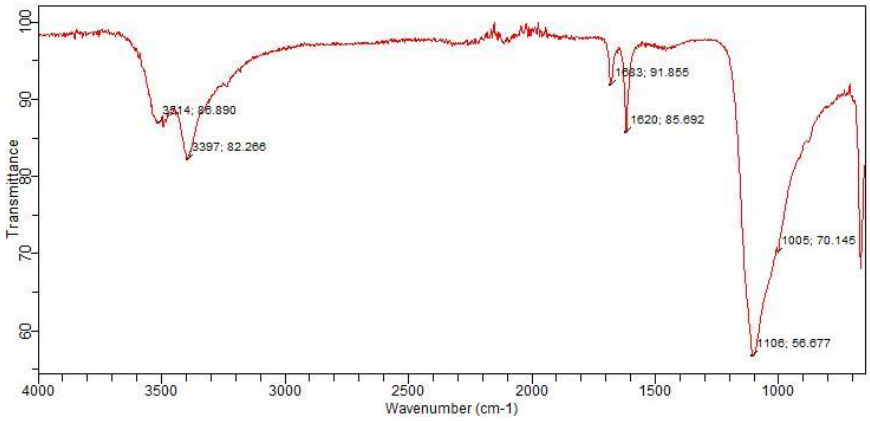

Figure 16: Spectrum of Sample H

Gypsum is prominently identified by characteristic O–H stretching bands around 3516 cm^{-1}, 3527 cm^{-1}, and 3627 cm^{-1}, reflecting the presence of structural water molecules intrinsic to the calcium sulfate dihydrate lattice [40, 41]. The H–O–H bending vibration near 1620 cm^{-1} further substantiates the hydration state of gypsum, confirming the retention of bound water critical to gypsum's crystalline structure and mechanical properties [41]. The sulfate vibrational modes at 1108 cm^{-1} and 1005 cm^{-1} correspond to SO_4^{2-} stretching and bending, respectively, which are hallmark signatures of gypsum mineral phases and influence the material's chemical stability and durability [20].

The glass fibers incorporated at 10g reveal their presence through broad Si–O–Si stretching bands spanning 1200–900 cm^{-1}, as well as distinct Si–O bending vibrations between 500–800 cm^{-1} [15, 43]. These bands indicate an amorphous silicate network characteristic of glass, which plays a crucial role in enhancing the composite's rigidity and resistance to environmental degradation [36]. The overlap of silicate bands with gypsum sulfate absorptions within the 1000–1100 cm^{-1} range is typical in such composites, highlighting the physical blending and interfacial interactions between the glass and gypsum phases [16].

PET, present at 5 g, is distinguished by ester carbonyl (C=O) stretching near 1715 cm^{-1} and C–O stretching vibrations in the 1240–1100 cm^{-1} region [34, 35]. While these PET-specific peaks partially overlap with sulfate and silicate bands, their clear presence confirms the polymer's integration into the composite. The aliphatic C–H stretching (typically seen near 2900 cm^{-1} but sometimes obscured) further supports the identification of PET [36]. The successful incorporation of PET imparts flexibility and toughness, counteracting gypsum's inherent brittleness and enhancing impact resistance [37].

The spectral overlaps observed between sulfate and silicate bands reflect the complex microstructural interactions and physical mixing rather than chemical bonding or degradation. This indicates that PET and glass fibers integrate well into the gypsum matrix without altering its fundamental chemical structure, preserving the composite's overall stability [16, 36]. The retention of key functional groups and the absence of new absorption bands suggest minimal chemical reaction between gypsum, PET, and glass during composite formation, corroborating findings by Malik *et al*. [34] who highlighted the importance of physical reinforcement over chemical modification in such composites.

These results align with prior research demonstrating FTIR spectroscopy's effectiveness in characterizing hybrid composite materials and assessing interfacial compatibility among components [35, 43]. The confirmed presence and compatibility of gypsum, PET, and glass fibers underscore the composite's potential for enhanced mechanical performance and environmental durability, making it suitable for construction and industrial applications where strength, flexibility, and moisture resistance are required [47].

CONCLUSION

The study revealed that reinforcing Plaster of Paris with waste polyethylene terephthalate and glass fibers improves its mechanical strength, toughness, and durability while reducing porosity, thus overcoming its inherent brittleness and weakness. SEM and FTIR analyses confirmed uniform dispersion and beneficial interfacial interactions at lower fiber loadings, though higher concentrations caused agglomeration and performance decline. Overall, these composites not only enhance the functional properties of POP for construction and decorative applications but also provide a sustainable pathway for recycling plastic and glass waste into value-added materials.

REFERENCES

[1] Sharma, R. & Prabu, V. (2013). Properties and Applications of Gypsum and Plaster of Paris. *Building and Environment*, 66, 135–142.

[2] Singh, P.& Verma, S. K. (2019). Impact of Waste Glass in Composites. *Journal of Materials in Civil Engineering*, 31(4), 04019013.

[3] Akinlabi, A. (2016). Basic Properties and Uses of Plaster of Paris in Building Construction. *Journal of Construction Materials Research*. 115(4), 489–498.

[4] Boyd, J. & Benjamin, J. (2015). Composite Materials: Fabrication Handbook. McGraw-Hill Education.

[5] Nepal, J., Dinesh, P. & Adhikari, M. (2022). Advantages of Composites Over Conventional Materials. *International Journal of Advanced Materials Research*, 9(2), 56–63.

[6] Fakirov, S. (2017). Handbook of Engineering Thermoplastics. Wiley-VCH.

[7] Britannica. (2023). Polyethylene Terephthalate (PET) Properties. Encyclopædia Britannica.

[8] Vince, K. (2020). PET in Construction Composites: A Review. *Journal of Advanced Materials Research*, 112(3), 57–66.

[9] Eko, S., Prasetyo, A. & Rahardjo, B. (2007). Management of Waste Glass: Challenges and Opportunities. *Waste Management Research*, 25(4), 401–405.

[10] Kaza, S., Yao, L., Bhada-Tata, P. & Woerden, F. V. (2018). What a Waste 2.0: A Global Snapshot of Solid Waste Management to 2050. World Bank.

[11] IUCN. (2023). Plastics: The World's Environmental Threat. International Union for Conservation of Nature.

[12] Noor, M. & Ahmed, K. (2020). Strengthening of POP Using Fibrous Reinforcements. *Construction and Building Materials*, 235, 117473.

[13] Zhang, H., Li, Q. & Sun, Z. (2019). Properties of Gypsum Composites Modified with Fibers. *Journal of Building Engineering*, 26, 100844.

[14] Benmokrane, B., El-Salakawy, E. & El-Ragaby, A. (2018). Fiber Reinforcement in Gypsum Composites. *Materials Journal*, 115(4), 489–498.

[15] Wang, Y., Zhang, Y. & Zhao, Q. (2020). Influence of silicate glass fillers on mechanical properties of gypsum composites. *Journal of Materials Science*, 55, 5278–5290. https://doi.org/10.1007/s10853-019-04236-7.

[16] Zhang, Y., Zhao, Q. & Wang, Y. (2021). Influence of phase transformation in gypsum-based materials on mechanical behavior and hydration process. *Journal of Materials in Civil Engineering*, 33(2), 04020468. https://doi.org/10.1061/(ASCE)MT.1943-5533.0003554

[17] Ahmad, S., Chen, B. & Wang, H. (2020). Mechanical properties of PET fiber-reinforced cement composites. *Construction and Building Materials*, 241, 118024

[18] Silva, D. A., Roman, H. R. & Gleize, P. J. (2005). The Use of PET Fibers in Mortars: Durability Evaluation. *Construction and Building Materials*, 19(7), 473–478.

[19] Sheikh, M. N. & Ashraf, M. (2021). Performance of Glass Fiber Reinforced Gypsum. Materials Today: *Proceedings*, 44, 1310–1314.

[20] Singh, A. & Garg, M. (2020). Mechanical Properties of POP-Based Composites. *Journal of Material Science Research*, 9(3), 91–100.

[21] Liu, W., Yu, Y. & Zhang, S. (2019). Porosity and mechanical performance of gypsum materials: Influence of compaction and particle morphology. *Construction and Building Materials*, 209, 353–362. https://doi.org/10.1016/j.conbuildmat.2019.03.141

[22] Roberto, B. (2020). The Role of PET in Packaging and Construction. *Polymer Science Journal*, 55(4), 287–297.

[23] Hlabano, M. M., Lukhele, B. & Ncube, M. (2018). Utilization of Sawdust Composite Panels. *Journal of Environmental and Earth Science*, 8(3), 22–30.

[24] Guna, V., Ravi, M. & Jaya, S. (2019). Use of Rice Husk Ash in Light Weight Ceiling Panels. *International Journal of Civil Engineering and Technology (IJCIET)*, 10(2), 55–62.

[25] Damanhur, E. A., Abdrabbo, F. M. & Mohamed, A. (2018). Rice husk composites for building panels. *Construction Research Journal*, 22(1), 54–62.

[26] Ugochukwu, U., Okorie, S. U. & Ukaegbu, I. K. (2019). Strengthening of POP with Kenaf Bast Fiber. *Journal of Material Cycles and Waste Management*, 21(2), 567–575.

[27] Barnett, S. (2005). Recycling of Glass Fiber Waste in Industry. Glass Research Institute Report.

[28] Sari, A., Karaipekli, A. & Kaygusuz, K. (2013). Thermal Energy Storage Materials for Building Envelopes. *Energy and Buildings*, 62, 24–32.

[29] Khalil, A. & El-Wazery, M. (2018). Water resistance of modified gypsum plaster composites. *Journal of Building Engineering*, 19, 132–141.

[30] Sair, S. (2019). Eco-friendly composites from cork and cardboard waste. *Journal of Cleaner Production*, 235, 643–652.

[31] Darmawan, I., Willy, O. & Budiman, J.A. (2020). Setting time of construction gypsum, dental plaster, and white orthodontic gypsum. *J Dent Res Dent Clin Dent Prospects*. 14(3), 167-170. Doi: 10.34172/joddd.2020.036. Epub 2020 Sep 21. PMID: 33408821; PMCID: PMC7770402.

[32] Melisa, M. & Dilşad, A. G., (2025). Development of Fe-reinforced PLA-based composite filament for 3D printing: Process parameters, mechanical and microstructural characterization, *Ain Shams Engineering Journal*. 16(2), 103279. https://doi.org/10.1016/j.asej.2025.103279.

[33] Zhou, Y., Wang, H. & Chen, L. (2019). Interfacial bonding and mechanical properties of fiber-reinforced gypsum composites. *Composites Part B: Engineering*, 164, 370–378. https://doi.org/10.1016/j.compositesb.2018.12.146

[34] Malik, M., Hassan, A. &Zakaria, M. (2020). Effect of glass fiber and plastic waste reinforcement on the mechanical and water absorption properties of hybrid composites. *Construction and Building Materials*, 247, 118453. https://doi.org/10.1016/j.conbuildmat.2020.118453

[35] Chowdhury, M. H., Hoque, M. M. & Rahman, M. M. (2020). Polymer-reinforced gypsum composites: A review of mechanical performance and durability. *Journal of Reinforced Plastics and Composites*, 39(4), 131–147. https://doi.org/10.1177/0731684419893942

[36] Rahman, M. M., Ahsan, Q., Hasan, M. &Hoque, M. M. (2019). Effect of hybrid fibers on the physical and mechanical properties of composite materials. *Materials Research Express*, 6(9), 095321. https://doi.org/10.1088/2053-1591/ab2a9e

[37] Mohammad, A. A., Alia, R. A. & Hussain, M. A. (2018). Phase transformation and mechanical properties of gypsum-based materials. *Materials Research Express*, 5(6), 065502.

[38] Mansour, N. A., Maher, A. &Hossam, H. (2020). Mechanical and morphological characterization of hybrid polymer–gypsum composites. Materials Today: *Proceedings*, **33**, 444–450. https://doi.org/10.1016/j.matpr.2020.05.327.

[39] Sahu, S., Acharya, B. & Roy, D. (2021). Microstructural and durability assessment of plaster-based composites for sustainable construction. *Journal of Building Engineering*, **35**, 102032. https://doi.org/10.1016/j.jobe.2020.102032

[40] Madejová, J. & Gates, W. P. (2017). FTIR techniques in clay mineral studies. *Developments in Clay Science*, 8, 177–231. https://doi.org/10.1016/B978-0-08-100369-1.00005-5

[41] Huang, Y., Li, X. & Sun, Y. (2021).FTIR analysis of gypsum and its hydrated phases under different curing conditions. *Construction and Building Materials*, 279, 122430. https://doi.org/10.1016/j.conbuildmat.2021.122430

[42] Li, S., Wu, Y. & Zhang, M. (2020). Influence of hydration water on the mechanical properties of gypsum-based materials: An FTIR and microstructural study. *Materials Science and Engineering A*, 787, 139494. https://doi.org/10.1016/j.msea.2020.139494

[43] Liang, J., Lu, J. & Zhao, L. (2018). Structural characterization of silicate glass particles by FTIR and Raman spectroscopy. *Journal of Non-Crystalline Solids*, 487, 1–9. https://doi.org/10.1016/j.jnoncrysol.2018.07.021

[44] Vola, A., Ferrara, L. & Berra, M. (2020). Waste glass in cement-based materials: Chemical interactions, microstructure, and properties. *Cement and Concrete Composites*, 114, 103758 https://doi.org/10.1016/j.cemconcomp.2020.103758

[45] Kuktaite, R., Skrifvars, M. & Hyvärinen, M. (2018). FTIR analysis of PET: Identification and degradation monitoring. *Polymers*, 10(6), 637. https://doi.org/10.3390/polym10060637

[46] Arefi, M. & Rezaei-Zarchi, S. (2012). The effect of using polypropylene fibers on physical and mechanical properties of gypsum composites. *Construction and Building Materials*, 36, 78–83. https://doi.org/10.1016/j.conbuildmat.2012.04.066

[47] Ogunleye, M. A. & Adewale, A. B. (2021). Recycled PET for Environmental Sustainability in Composites. *Environmental Challenges*, 4, 100138.